SHOCK WAVE INCIDENCE ON A V-SHAPED CAVITY

S. K. Godunov, Ya. M. Kazhdan,
and V. A. Simonov

We study theoretically and experimentally the motion of metal arising from a plane shock wave striking a V-shaped cavity. Using the functionally invariant solutions of Sobolev, we write out the acoustic approximation for this problem and determine the region of its applicability. It is shown that in the region in which the acoustic approximation is not applicable, the flow in the principal term is described by the incompressible fluid equations for which the boundary conditions are defined by the acoustic region. The experimental technique is described and a comparison of the theoretical and experimental data is made.

We examine the motion which develops as a result of incidence of a shock wave, parallel to the xz plane, on a V-shaped cavity whose apex coincides with the z axis. The equation of state of the medium is

$$p = \frac{\rho_0 c_0^2}{\varkappa}(\delta^{\varkappa}\gamma - 1) \tag{1}$$

Ahead of the wave the velocity u = 0, pressure p = 0, relative density $\delta = 1$, the entropy measure $\gamma = 1$, the density is ρ_0, and the sound speed is c_0. The constant pressure p_1 is specified at the shock wave front. The study is made under the assumption that the ratio

$$\varepsilon = \frac{p_1}{\rho_0 c_0^2} \tag{2}$$

is small.

In this case it turns out that the flow examined in the principal term in x, y, z, t space breaks down into two regions: in the first region, immediately adjacent to the front, the principal term is determined by the linearized equations of gasdynamics (acoustic approximation), while in the second region the principal term is determined by the incompressible fluid equations. In the following, we present the principal term in the region corresponding to the acoustic approximation and establish the region in which the principal flow term is determined by the incompressible fluid equations.

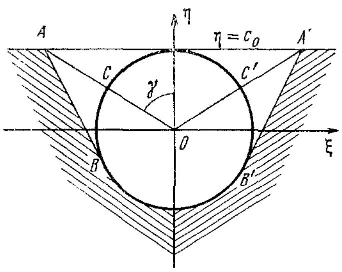

Fig. 1

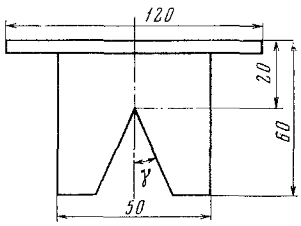

Fig. 2

Moscow. Translated from Zhurnal Prikladnoi Mekhaniki i Tekhnicheskoi Fiziki, Vol. 10, No. 6, pp. 57-61, November-December, 1969. Original article submitted May 28, 1969.

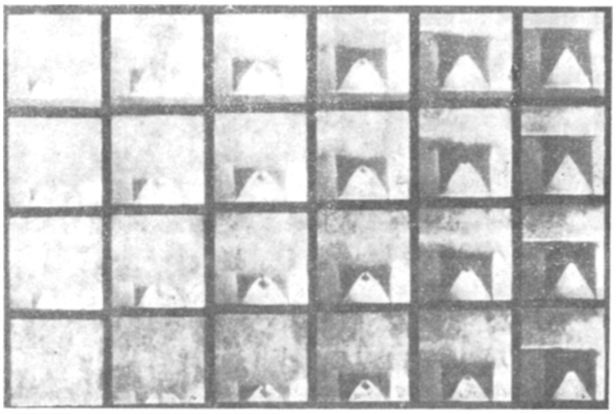

Fig. 3

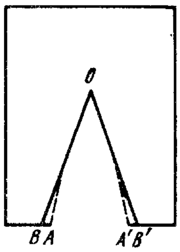

Fig. 4

It is obvious that the flow is independent of the z coordinate; therefore, we examine the flow in the x, y plane. It follows from the conditions at the shock wave that at the front

$$p_1 = \rho_0 c_0^2 \varepsilon, \quad \delta = 1 + \varepsilon, \quad u_x = 0, \quad u_y = \varepsilon c_0, \quad D = c_0 \tag{3}$$

where D is the wave velocity.

At the front $u/c_0 \approx \varepsilon$. As long as this ratio remains small, we can consider the acoustic approximation; in this approximation we can assume that

$$p = \rho_0 c_0^2 (\delta - 1) \tag{4}$$

The linearized gasdynamic equations are

$$\frac{\partial p}{\partial t} + \rho_0 c_0^2 \left(\frac{\partial u_x}{\partial x} + \frac{\partial u_y}{\partial y}\right) = 0, \quad \frac{\partial u_x}{\partial t} + \frac{1}{\rho_0}\frac{\partial p}{\partial x} = 0, \quad \frac{\partial u_y}{\partial t} + \frac{1}{\rho_0}\frac{\partial p}{\partial y} = 0 \tag{5}$$

The motion behind the front after its incidence on the hollow wedge is self-similar. The self-similar variables are $\xi = x/t$, $\eta = y/t$ (t is time reckoned from the moment of incidence). The line $\eta = c_0$ corresponds to the shock wave front. The equations of motion in the acoustic approximation coincide with the equations written in Lagrangian coordinates. Therefore, in the acoustic approximation the free boundary coincides with the sides of the wedge, i.e.,

$$\xi = \pm \mathrm{tg}\, \gamma \eta \ (2\gamma \text{ is the wedge angle}). \tag{6}$$

In the ξ, η plane, outside the region cut out by the characteristics emanating from the points where the front crosses the free boundary, the values of the gasdynamic functions coincide with the corresponding values at the front. In the variables ξ, η the acoustic equations will be

$$\frac{\partial \delta}{\partial \xi}\xi + \frac{\partial \delta}{\partial \eta}\eta - \left(\frac{\partial u_x}{\partial \xi} + \frac{\partial u_y}{\partial \eta}\right) = 0, \quad \frac{\partial u_x}{\partial \xi}\xi + \frac{\partial u_x}{\partial \eta}\eta - c_0^2 \frac{\partial \delta}{\partial \xi} = 0, \quad \frac{\partial u_y}{\partial \xi}\xi + \frac{\partial u_y}{\partial \eta}\eta - c_0^2 \frac{\partial \delta}{\partial \eta} = 0 \tag{7}$$

The flow characteristics will be the straight lines

$$\eta = C\xi \tag{8}$$

corresponding to the streamlines, the straight lines

$$\eta = p\xi \pm \sqrt{1 + p^2}\, c_0 \tag{9}$$

and the circular arc enveloping them

$$\xi^2 + \eta^2 = c_0^2 \tag{10}$$

The region of constancy is bounded by the front $\eta = c_0$, and by the characteristics AB, A'B', BB'. (Shaded region in Fig. 1.)

The equation of the characteristic AB is

$$\eta = \pm [\mathrm{tg}\, 2\gamma\xi - c_0 \sqrt{1 + \mathrm{tg}^2 2\gamma}] (+ \sim \gamma < 1/4\pi, \ - \sim \gamma > 1/4\pi) \tag{11}$$

The equation of the characteristic A'B' is

$$\eta = \pm [\mathrm{tg}\, 2\gamma\xi - c_0\sqrt{1 + \mathrm{tg}^2 2\gamma}] \quad (- \sim \gamma < 1/4\pi, \ + \sim \gamma > 1/4\pi) \tag{12}$$

In Fig. 1 the broken line BACOC'A'B' and the circular arc BB' bound on the plane of the self-similar variables ξ, η the zone disturbed by the wave which reflects from the cutout boundary. In this region the flow is potential. The solution of the acoustics equations in this region was first calculated by Sobolev [1] using functionally invariant solution theory.

After introducing the potential φ in the form

$$\varphi(x, y, t) = t\Phi(\xi, \eta) \tag{13}$$

this solution can be written as

$$\begin{aligned} &\Phi = 0 \text{ on free boundary } OA \text{ and } OA' \\ &\Phi = -c_0^2\varepsilon\,[\sin 2\gamma\xi - (1 - \cos 2\gamma)\eta] \ \text{ in region } C'A'B' \\ &\Phi = c_0^2\,\varepsilon\,[\sin 2\gamma\xi - (1 - \cos 2\gamma)\eta] \ \text{ in region } CAB \\ &\Phi = \Phi_0(\xi, \eta) \text{ in region } COC'B'BC \end{aligned} \tag{14}$$

Here

$$\Phi_0 = \sum_{n=0}^{\infty} C_n \left(\frac{r}{1 + \sqrt{1 - r^2}}\right)^{2(n+1)\alpha} [1 + (2n + 1)\alpha\sqrt{1 - r^2}]\cos(2n + 1)\alpha(\pi - \theta)$$

$$C_n = (-1)^n \frac{16(\pi - \gamma)^2 c_0^2\varepsilon\cos(2n + 1)\alpha\gamma}{(2n + 1)[(2n + 1)^2\pi^2 - 4(\pi - \gamma)^2]}, \qquad \alpha = \frac{\pi}{2(\pi - \gamma)} \tag{15}$$

$$r = \frac{\sqrt{\xi^2 + \eta^2}}{c_0}, \qquad \theta = \mathrm{arc\,tg}\frac{\xi}{\eta}, \quad u_x = \frac{\partial\Phi}{\partial\xi}, \qquad u_y = \frac{\partial\Phi}{\partial\eta} \tag{16}$$

From the first and second equations (7) and the condition $\Phi = 0$ at the free boundary, it follows that

$$c_0^2(\delta - 1) = \xi\partial\Phi/\partial\xi + \eta\partial\Phi/\partial\eta - \Phi = r\partial\Phi/\partial r - \Phi \tag{17}$$

The series defining δ can be summed

$$\begin{aligned} &\delta = 1 + \varepsilon\left[\mathrm{arc\,tg}\frac{\cos\alpha(\gamma + \pi - \theta)}{\mathrm{sh}\,\alpha q} + \mathrm{arc\,tg}\frac{\cos\alpha(\gamma + \pi + \theta)}{\mathrm{sh}\,\alpha q}\right] \\ &q = \ln(1 + \sqrt{1 - r^2}) - \ln r \end{aligned} \tag{18}$$

In the present paper we draw certain qualitative conclusions from these formulas and compare them with experiment.

It follows from (15) and (18) that as $r \to 0$

$$\frac{\partial\Phi}{\partial r} \approx 4c_0^2\frac{\alpha}{\alpha - 1}\varepsilon\cos\alpha\gamma\cos\alpha(\pi - \theta)\, r^{\alpha-1}, \quad \frac{\partial\Phi}{\partial\theta} \approx 4c_0^2\frac{\alpha}{\alpha - 1}\varepsilon\cos\alpha\gamma\sin\alpha(\pi - \theta)\, r^{\alpha}$$
$$\delta - 1 \approx 4\varepsilon\cos\alpha\gamma\cos\alpha(\pi - \theta) r^{\alpha} \tag{19}$$

The solution (15), (18) therefore corresponds to the acoustic approximation but is valid only in the region in which the particle velocity is small in comparison with the sound speed. As $r \to 0$

$$v^2 = \frac{1}{c_0^2}\left[\left(\frac{\partial\Phi}{\partial r}\right)^2 + \frac{1}{r^2}\left(\frac{\partial\Phi}{\partial\theta}\right)^2\right] \approx \frac{16c_0^2\alpha^2}{(\alpha - 1)^2}\varepsilon^2 r^{2(\alpha-1)} \tag{20}$$

Since $1/2 < \alpha < 1$, as $r \to 0$, the value of $v^2 \to \infty$; therefore, it is necessary to identify the region in which the acoustic approximation is valid. As a result of substituting the asymptotic expression (19) into the linearized gasdynamic equations for isentropic and potential flows, we find that the acoustic approximation can be used only in that region where $\varepsilon r^{\alpha-2} \ll 1$. To study the solution in the region where $\varepsilon r^{\alpha-2} \approx 0(1)$, it is convenient to convert to the new scales

$$r = \varepsilon^{1/(2-\alpha)} R, \qquad \Phi = \varepsilon^{2/(2-\alpha)}\psi, \qquad \delta - 1 = \varepsilon^{2/(2-\alpha)}\Delta \tag{21}$$

In this case the region of finite values of R is subject to investigation. Approach of r to 0 in the acoustic region means that $R \to \infty$. Consequently, as $R \to \infty$ the following asymptotic relation is valid:

$$\psi \approx \frac{4c_0^2}{\alpha - 1} \cos \alpha\gamma \cos \alpha\theta R^\alpha, \qquad \Delta = 4 \cos \alpha\gamma \cos \alpha\theta R^\alpha \tag{22}$$

It follows from the equations obtained by substituting (21) into the gasdynamic system for isentropic and potential flows that as $\varepsilon \to 0$ and for finite values of R the following equation must be satisfied:

$$\frac{\partial^2 \psi}{\partial R^2} + \frac{1}{R^2} \frac{\partial^2 \psi}{\partial \theta^2} + \frac{1}{R} \frac{\partial \psi}{\partial R} = 0 \tag{23}$$

i.e., $\psi(R, Q)$ is a harmonic function satisfying the asymptotic relation

$$\psi \approx \frac{4c_0^2}{\alpha - 1} \cos \alpha\gamma \cos \alpha\theta R^\alpha \quad \text{for} \quad R \to \infty \tag{24}$$

Since the acoustic approximation ceases to be valid for finite values of R, the free boundary in the ξ, η plane no longer coincides with the straight-line segments. Along the free boundary the following equations must be satisfied:

$$\frac{\partial x}{\partial t} = u, \qquad \frac{\partial y}{\partial t} = v, \qquad \frac{\partial \varphi}{\partial t} + \frac{1}{2} v^2 = 0 \tag{25}$$

which in the variables ξ, η and the function $\psi(\xi, \eta)$ is written as

$$\frac{\partial \eta}{\partial \xi} = \left(\frac{\partial \psi}{\partial \eta} - \eta\right) \Big/ \left(\frac{\partial \psi}{\partial \xi} - \xi\right), \quad \psi - \psi_\xi \xi - \psi_\eta \eta + \frac{1}{2}(\psi_\xi^2 + \psi_\eta^2) = 0 \tag{26}$$

We note, incidentally, that the boundary condition (26) yields the same scale for transition from the region where acoustics governs into the region in which the incompressible fluid equations appear in the principal term.

Obviously, as $R \to \infty$ the equation of the free boundary will be

$$\xi \approx \pm \operatorname{tg} \gamma\eta \tag{27}$$

Thus the problem is reduced to finding the harmonic function $\psi(\lambda, \eta)$ which satisfies the asymptotic relation (24) and the conditions at the free boundary (26).

The experimental study of the process of shock wave incidence on a corner was accomplished with the aid of the SFR high-speed photorecorder operating in the time magnification regime with frame rate 10^6 per second. The experiments were conducted in dural specimens with the dimensions shown in Fig. 2. Explosive charges made from hexogen and TG 50/50 were used as the shock wave sources. Special conical charges made from two explosives with different detonation rates were prepared in order to obtain a plane shock wave. The charges were placed directly on the upper surface of the specimen.

The angles γ at the apex of the observed wedge were 15, 30, 32°. Figure 3 shows photographs of the jet formation process for the angles $\gamma = 15°$ and $\gamma = 32°$.

In comparing the results of the theoretical study and the experimental data, we compared the velocities w of the motion of the point of intersection of the free boundary with the axis of symmetry, the "collapse" point, and the free boundary profile. In the acoustic approximation the quantities r and θ can be considered the Lagrangian coordinates and we can use (22) to find the Eulerian coordinates of a given point. The correspondence between the Eulerian and Lagrangian coordinates will not be one-to-one in the vicinity of the collapse point. This is associated with the fact that the acoustic approximation is not applicable in this vicinity. Specifically, the half-lines corresponding to the free boundary become two curves which cross on the axis of symmetry. The point of intersection of these curves can be taken as the collapse point, and the curve segments located below this point can be taken as the free boundary profile. We note that the free-boundary profile obtained in this way will change with time; however, the angle formed by the profile with the axis of symmetry at the collapse point does not depend on the time. The following comparative data describe the velocities w of the collapse point O, and Fig. 4 shows the free-boundary profiles obtained experimentally for $t = \infty$ (B'OB), and from the acoustic approximation (dashed line A'OA) for some definite value of t.

For $\gamma = 15°$ the calculated w = 9000 m/sec, experimental w = 7000–8000 m/sec; for $\gamma = 30°$ the calculated w = 7000 m/sec, experimental w = 6000–8000 m/sec.

The authors wish to thank A. A. Deribas for discussion on the problem formulation and experimental technique, and N. S. Kozin for carrying out the numerical calculations.

LITERATURE CITED

1. S. L. Sobolev, "Theory of plane wave diffraction," Tr. seismologicheskogo in-ta, no. 41, 1934.